

Low-Energy Polymeric Phases of Alanates

Tran Doan Huan,¹ Maximilian Amsler,¹ Miguel A. L. Marques,²
Silvana Botti,² Alexander Willand,¹ and Stefan Goedecker^{1,*}

¹*Department of Physics, Universität Basel, Klingelbergstrasse 82, 4056 Basel, Switzerland*

²*Université de Lyon, F-69000 Lyon, France and LPMC, CNRS,
UMR 5586, Université Lyon 1, F-69622 Villeurbanne, France*

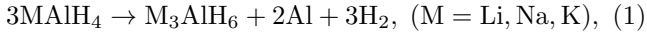
(Dated: November 6, 2012)

Low-energy structures of alanates are currently known to be described by patterns of isolated, nearly ideal tetrahedral $[\text{AlH}_4]$ anions and metal cations. We discover that the novel polymeric motif recently proposed for LiAlH_4 plays a dominant role in a series of alanates, including LiAlH_4 , NaAlH_4 , KAlH_4 , $\text{Mg}(\text{AlH}_4)_2$, $\text{Ca}(\text{AlH}_4)_2$ and $\text{Sr}(\text{AlH}_4)_2$. In particular, most of the low-energy structures discovered for the whole series are characterized by networks of corner-sharing $[\text{AlH}_6]$ octahedra, forming wires and/or planes throughout the materials. Finally, for $\text{Mg}(\text{AlH}_4)_2$ and $\text{Sr}(\text{AlH}_4)_2$, we identify two polymeric phases to be lowest in energy at low temperatures.

PACS numbers: 61.66.-f, 63.20.dk, 61.05.cp

Hydrogen is a compelling alternative to fossile fuels as it can deliver clean energy and is readily available in large quantities. Solid state hydrides for hydrogen storage as intended on board of vehicles need to provide high gravimetric hydrogen density ($\gtrsim 5.5$ % wt), reasonable decomposition temperatures ($\lesssim 100^\circ \text{C}$), and full reversibility [1, 2]. Tremendous research efforts have been devoted to metal alanates $\text{M}(\text{AlH}_4)_n$ (where M is a metal cation of valence n) as promising candidates. At low temperatures, alanates are known to crystallize in phases which are characterized by patterns of isolated, nearly ideal tetrahedral $[\text{AlH}_4]^-$ anions and M^{n+} cations [3–16]. Recently, low-energy phases were predicted for LiAlH_4 with a novel structural motif [17]. In these phases, networks of corner-sharing $[\text{AlH}_6]$ octahedra form wires and planes throughout the material. We will hereafter refer to such phases as “polymeric phases” while the expression “isolated phases” will be used for structures characterized by isolated $[\text{AlH}_4]$ tetrahedra.

The discovery of energetically favorable polymeric phases in LiAlH_4 may have an impact on the controversy over the stability of this compound [4, 18, 19]. Furthermore, the $[\text{AlH}_6]$ octahedra may influence the kinetics of the dehydrogenation process [20, 21]



since the same $[\text{AlH}_6]$ octahedra have been reported in Li_3AlH_6 [4, 22]. This behavior could be transferred to other alanates and may be helpful in for example improving their stability at ambient conditions, e.g. $\text{Mg}(\text{AlH}_4)_2$ [8, 9]. Also, the $[\text{AlH}_6]$ octahedra have been observed in the dehydrogenation products of many other alanates, such as Na_3AlH_6 [23] and K_3AlH_6 [14, 21] from NaAlH_4 and KAlH_4 via reaction (1), and CaAlH_5 and SrAlH_5 from $\text{Ca}(\text{AlH}_4)_2$ and $\text{Sr}(\text{AlH}_4)_2$ via reaction (2), respectively [10, 16, 24–27]



These similarities strongly suggest that polymerization of $[\text{AlH}_4]$ in alanates may influence the dehydrogenation processes of such compounds.

In this Letter, we investigate the low-energy polymeric phases of a series of six alanates, including three alkali metal alanates LiAlH_4 , NaAlH_4 , KAlH_4 , and three alkaline earth metal alanates $\text{Mg}(\text{AlH}_4)_2$, $\text{Ca}(\text{AlH}_4)_2$, $\text{Sr}(\text{AlH}_4)_2$. The first-principles calculations in this work were performed at the density functional theory (DFT) [28, 29] level using the ABINIT package [30–32]. We used the generalized gradient approximation, the Perdew-Burke-Ernzerhof (PBE) exchange-correlation functional [33] and the norm-conserving Hartwigsen-Goedecker-Hutter pseudopotentials [34] for total energy and linear response phonon calculations. The plane-wave cutoff energy was 60 hartree (Ha) while a Monkhorst-Pack \mathbf{k} -point mesh [35] was chosen for each structure, ensuring the convergence of the total energy to be better than 10^{-5} Ha/atom. Atomic and cell variables were simultaneously relaxed until all the residual force and stress components were smaller than 10^{-5} Ha \times bohr $^{-1}$ and 10^{-7} Ha \times bohr $^{-3}$, respectively. Additional calculations with PBEsol [36] and LDA exchange-correlation functionals were performed to confirm the energetic orderings of the phases.

The recently generalized minima-hopping method (MHM) [37, 38] was used to predict novel crystal structures. The DFT-energy landscape is thereby explored by short consecutive molecular dynamics steps followed by local geometry relaxations. The initial velocities for the molecular dynamics runs are chosen approximately along soft mode directions, allowing efficient escapes from local minima, and aiming toward the global minimum. The predictive power of the MHM has already been demonstrated in a wide range of applications [17, 39–45].

We performed several MHM simulations with up to 4 formula units (f.u.) per cell for LiAlH_4 , NaAlH_4 and KAlH_4 , and with up to 2 f.u. per cell for $\text{Mg}(\text{AlH}_4)_2$,

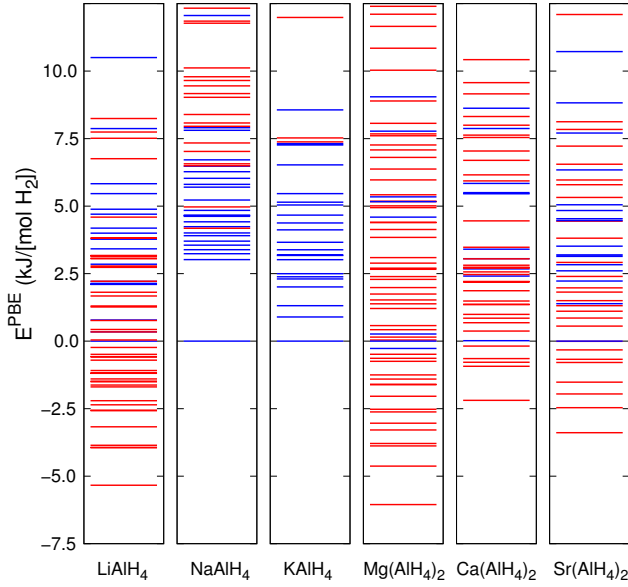


FIG. 1. (Color online) Low-energy spectra of LiAlH_4 , NaAlH_4 , KAlH_4 , $\text{Mg}(\text{AlH}_4)_2$, $\text{Ca}(\text{AlH}_4)_2$ and $\text{Sr}(\text{AlH}_4)_2$. Blue/red lines represent the isolated/polymeric phases. Energies are given in unit of $\text{kJ}/[\text{mol H}_2]$ with respect to those of the reference phases (see the text).

$\text{Ca}(\text{AlH}_4)_2$, and $\text{Sr}(\text{AlH}_4)_2$, starting from random input structures. For a given number of formula units per primitive cell, our runs were able to recover all of the previously reported isolated phases of the alanates, which belong to the space group $P2_1/c$ for LiAlH_4 [3, 4], $I4_1/a$ for NaAlH_4 [5], $Pnma$ for KAlH_4 [6], and $P\bar{3}m1$ for $\text{Mg}(\text{AlH}_4)_2$ [7, 8]. The $Pcba$ phase for $\text{Ca}(\text{AlH}_4)_2$ [10] could obviously not be found since it has 8 f.u. per primitive cell. For $\text{Sr}(\text{AlH}_4)_2$, there are no conclusive crystallographic information available in literature to our best knowledge [16].

Furthermore, we discovered a large number of novel low-energy structures for all the compounds. The energy spectra of these phases are shown in Fig. 1 (without zero-point correction E_{ZP}) with respect to the reference structures, chosen to be the most stable reported isolated phases. For $\text{Sr}(\text{AlH}_4)_2$, the lowest isolated phase (space group $P\bar{1}$) from our predictions in $\text{Sr}(\text{AlH}_4)_2$ was used as reference [46]. Although several polymeric phases were found for NaAlH_4 and KAlH_4 , their most stable phases are isolated. On the other hand, a large number of polymeric phases were discovered for LiAlH_4 , $\text{Mg}(\text{AlH}_4)_2$, $\text{Ca}(\text{AlH}_4)_2$, and $\text{Sr}(\text{AlH}_4)_2$, dominating their low-energy configurational space. The geometry of the most stable polymeric phase for each alanate is shown in Fig. 2.

A summary of the energetic and structural properties of the most stable polymeric phases is given in Table I (see also Supplemental Material [46]). For these structures, the total energies E^{PBE} , E^{PBEsol} , and E^{LDA} were

TABLE I. Summary of the three most stable polymeric phases of each alanate. Total energies E^{PBE} , E^{PBEsol} and E^{LDA} are obtained with PBE, PBEsol, and LDA exchange-correlation functionals. Zero-point energies E_{ZP} are included in $E_{\text{ZP}}^{\text{PBE}}$. The energies are given in unit of $\text{kJ}/[\text{mol H}_2]$ with respect to the reference phases. Space group numbers are given in parentheses.

Compound	Space group	E^{PBE}	$E_{\text{ZP}}^{\text{PBE}}$	E^{PBEsol}	E^{LDA}
LiAlH_4	$P2_1/c$ (14)	-5.32	-3.07	-12.15	-12.38
	$P2_1$ (4)	-3.94	-1.65	-11.12	-11.33
	$Pnc2$ (30)	-3.92	-1.49	-11.44	-11.72
NaAlH_4	$C2/m$ (12)	4.07	5.28	3.31	2.67
	$P\bar{1}$ (2)	5.03	6.66	3.89	3.81
	$C2$ (5)	6.30	7.57	5.32	0.21
KAlH_4	$P\bar{1}$ (2)	7.37	10.45	0.84	-0.37
	$Ama2$ (40)	7.56	10.00	3.70	3.60
	$Cmcm$ (63)	11.99	14.01	5.56	3.69
$\text{Mg}(\text{AlH}_4)_2$	$P2_1$ (4)	-6.07	-2.53	-16.29	-18.38
	$P2$ (3)	-4.59	-0.79	-13.88	-16.74
	$C2/m$ (12)	-3.89	-0.09	-12.84	-15.07
$\text{Ca}(\text{AlH}_4)_2$	$P2_1/c$ (14)	-2.17	0.48	-12.15	-14.26
	$C2$ (5)	-0.85	1.72	-11.04	-13.19
	Pm (6)	-0.77	1.86	-11.74	-14.54
$\text{Sr}(\text{AlH}_4)_2$	Pm (6)	-3.49	-1.18	-8.94	-9.70
	$P2_1/c$ (14)	-2.56	-0.67	-5.85	-5.70
	$P\bar{1}$ (2)	-2.05	0.38	-6.75	-7.30

obtained with the PBE, PBEsol, and LDA exchange-correlation functionals, respectively, while E_{ZP} was calculated with the PBE functional and included in $E_{\text{ZP}}^{\text{PBE}}$. Without E_{ZP} , the energetic orderings are invariant with respect to the different employed exchange-correlation functionals. However, E_{ZP} was found to be important and may change the energetic orderings, i.e., with E_{ZP} , the most stable phases of NaAlH_4 ($I4_1/a$), KAlH_4 ($Pnma$), and $\text{Ca}(\text{AlH}_4)_2$ ($Pbca$) are isolated while the most stable phases of LiAlH_4 ($P2_1/c$), $\text{Mg}(\text{AlH}_4)_2$ ($P2_1$), and $\text{Sr}(\text{AlH}_4)_2$ (Pm) are polymeric. The simulated X-ray diffraction spectra were compared to experimental results and can be found in the Supplemental Materials [46].

The $[\text{AlH}_6]$ octahedra in all polymeric phases share the same geometrical structure: the Al atom at the center is surrounded by four H atoms on a plane while the other two H atoms form Al-H bonds nearly perpendicular to the plane. In polymeric phases the negatively charged $[\text{AlH}_6]$ octahedra are linked together by sharing their corners to form networks of wires and/or planes throughout the material. To estimate the charge transfer onto the $[\text{AlH}_6]$ polymers, we performed a Bader charge analysis calculation on the $P2_1$ phase of $\text{Mg}(\text{AlH}_4)_2$ and on the Pm phase of $\text{Sr}(\text{AlH}_4)_2$ using the AIM utility of the ABINIT package. We found that a charge of $-1.65q_e$ and $-1.36q_e$ is transferred from a Mg and Sr atom to the

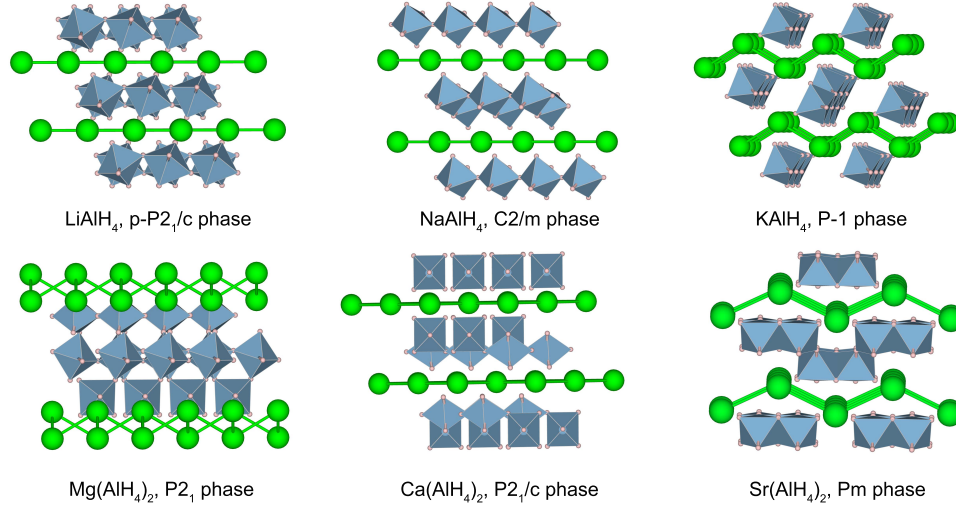


FIG. 2. (Color online) Most stable polymeric phases of LiAlH_4 , NaAlH_4 , KAlH_4 , $\text{Mg(AlH}_4)_2$, $\text{Ca(AlH}_4)_2$, and $\text{Sr(AlH}_4)_2$. Green spheres represent metal cations while octahedra are formed by $[\text{AlH}_6]$ complexes. Space groups are also given.

$[\text{AlH}_6]$ complexes, respectively, clearly indicating that the polymeric sub-structures themselves carry a strong electric charged.

We further analyzed structural and energetic relationships between the alanes. For three lowest-energy phases of each alane, we replaced the cation by the two other cations of same valence, and then a small step-size local geometry relaxation was performed. The energetic ordering of the relaxed structures is shown in Fig. 3. There is no clear rank correlation of the three alanes within a group. We obtained a geometric average of $\tau = 0.47$ for the Kendall tau rank correlation for the group of monovalent metal alanes and $\tau = 0.44$ for the divalent group. In particular, the ground state structures are completely unrelated with each other. Therefore, database searching methods which are often based

on exchanging cations of ground state phases in another compound are bound to fail to predict the correct structure, emphasizing the need for unconstrained and systematic structure prediction algorithms.

In order to investigate the dynamical stability we performed linear response phonon calculations for all the polymeric phases shown in Table I. No imaginary phonon modes were observed in the whole Brillouin zones, indicating that all phases are dynamically stable. The zero-temperature densities of phonon states $\rho_{\text{ph}}(\omega)$ of these phases are given in the Supplemental Material [46]. The partial and total densities of phonon states of the polymeric P2_1 phase and the isolated $\text{P}\bar{3}m1$ phase of

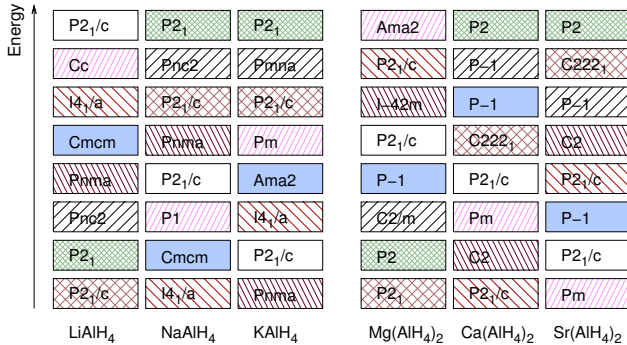


FIG. 3. (Color online) Energetic ordering and space groups of the structures obtained by substituting the cations of the alanes within a group. For each of the two groups ($\text{M}=\text{Li}$, Na , K and $\text{M}=\text{Mg}$, Ca , Sr) structures with identical colors and patterns have the same origin.

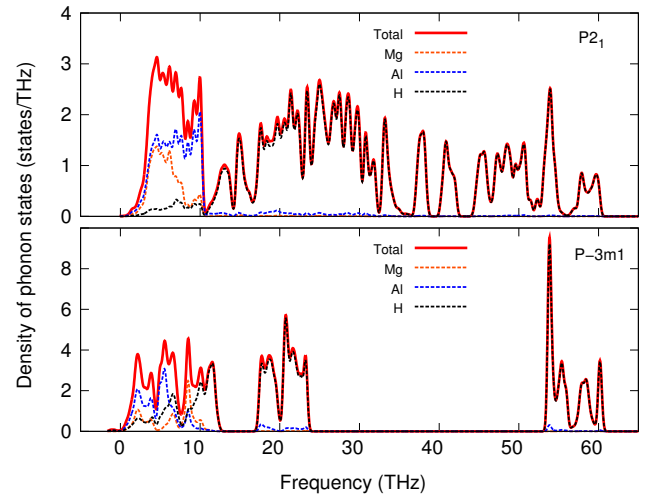


FIG. 4. (Color online) Densities of phonon states (partial and total) for 2 f.u. of $\text{Mg(AlH}_4)_2$ in P2_1 and $\text{P}\bar{3}m1$ phases.

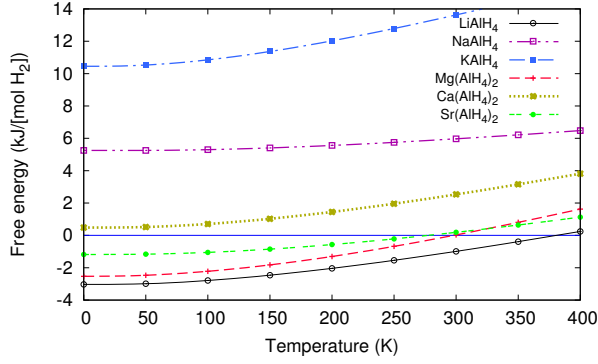


FIG. 5. (Color online) Free energy of the lowest polymeric structures of the aluminates, given with respect to that of the corresponding isolated reference structures.

$\text{Mg}(\text{AlH}_4)_2$ are compared in Fig. 4. In both phases, three frequency ranges (below 12 THz, 12 – 40 THz, and above 40 THz) correspond to the Mg/Al framework vibrations, the molecular libration and Al-H bending modes, and the Al-H stretching modes, respectively. Because the $[\text{AlH}_4]$ tetrahedra in the $P\bar{3}m1$ phase are isolated and essentially independent, these frequency ranges are localized in narrow energy windows and are clearly distinct. On the other hand, the librational/Al-H bending frequencies and the Al-H stretching frequencies of the $P2_1$ phase are smeared out in a wide energy range. This behavior is a consequence of the polymeric motifs of the $[\text{AlH}_6]$ octahedra, which are linked together by the H atoms at several corners. Therefore, the contribution of the zero-point vibrational energy at 0 K of any polymeric phase, quantified by $E_{\text{ZP}} \equiv \int_0^\infty d\omega \left[\frac{\omega}{2} \rho_{\text{ph}}(\omega) \right]$, is larger than in isolated phases, as shown in Table I.

At finite temperatures, the significance of the vibrational energy becomes even more apparent. Fig. 5 shows the free energies of the most stable polymeric phases of the aluminates, given with respect to the reference phases. All polymeric phases become monotonically less (thermodynamically) stable as the temperature increases. This behavior demonstrates that the vibrational contribution to the free energy of any polymeric phase grows faster than in the corresponding isolated reference phase. For LiAlH_4 , $\text{Mg}(\text{AlH}_4)_2$, and $\text{Sr}(\text{AlH}_4)_2$, the $P2_1/c$, $P2_1$, and Pm phases become less stable than the corresponding reference phases above 380K, 300K, and 280 K, respectively. On the other hand, the $P2_1$ phase of $\text{Mg}(\text{AlH}_4)_2$ could enhance the stability of $\text{Mg}(\text{AlH}_4)_2$ which has been reported to be metastable at ambient conditions in the $P\bar{3}m1$ phase [8, 9].

Furthermore, we investigated the electronic properties of two polymeric phases and performed *GW* calculations [47] for the $P2_1$ phase of $\text{Mg}(\text{AlH}_4)_2$ and the Pm phase of $\text{Sr}(\text{AlH}_4)_2$, and their corresponding reference phases. The polymeric $P2_1$ phase was found to be an

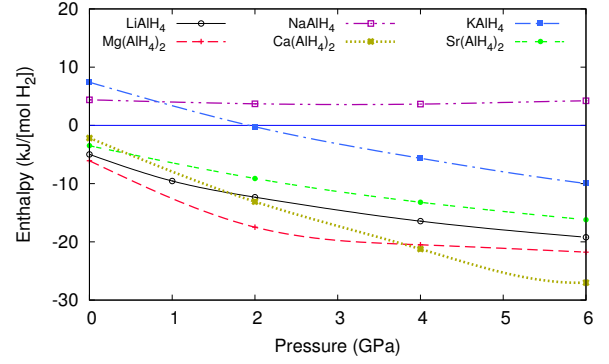


FIG. 6. (Color online) Enthalpies as a function of pressure for the lowest polymeric structures with respect to the corresponding isolated reference phases.

insulator with an indirect band-gap of 4.7 eV, which is significantly lower than that of the isolated $P\bar{3}m1$ phase, determined to be 6.5 eV in agreement with previous results [8, 9]. For $\text{Sr}(\text{AlH}_4)_2$, we found that the Pm phase is also an insulator with a gap of 5.3 eV.

Finally, Fig. 6 demonstrates that the profound differences in the structural motifs of the polymeric and isolated phases also have a strong influence on their compressibility and relative thermodynamical stability upon compression. It shows the pressure evolution of the enthalpies of the lowest polymeric structures with respect to the reference phases. As already indicated in Ref. [17] for the case of LiAlH_4 , the stability of the polymeric phases improves drastically as the pressure increases, with the exception of NaAlH_4 . In particular, the isolated phase in KAlH_4 is predicted to transform into a polymeric phase at a pressure of 2 GPa and 0 K. Therefore, cold compression of aluminates could be a promising approach en route to experimental synthesis of polymeric phases.

In conclusion, we unveiled the complexity of the energy landscape in several aluminates and the dominant role of the recently-proposed polymeric phases in their low-energy polymorphs. These polymeric phases are characterized by a charged network of corner-sharing $[\text{AlH}_6]$ octahedra and a significant vibrational energy. Two insulating polymeric phases of $P2_1$ and Pm symmetries were identified to be the most stable in $\text{Mg}(\text{AlH}_4)_2$ and $\text{Sr}(\text{AlH}_4)_2$. Both free energy and enthalpy calculations show that such phases should in fact be possible to synthesize, either at low temperatures or at high pressures. However, further experimental investigations are necessary to attain a deeper understanding of such structural properties in aluminates.

The authors thank Nguyen-Manh Duc for useful discussions. TDH, MA, AW, and SG acknowledge the financial support provided by the Swiss National Science Foundation. Computational resources were provided by the Swiss National Supercomputing Center (CSCS) in

Lugano.

* stefan.goedecker@unibas.ch

- [1] L. Schlapbach and A. Züttel, *Nature* **414**, 353 (2001).
- [2] T. K. Mandal and D. H. Gregory, *Annu. Rep. Prog. Chem., Sect. A* **105**, 21 (2009).
- [3] B. C. Hauback, H. W. Brinks, and H. Fjellvåg, *J. Alloys Compd.* **346**, 184 (2002).
- [4] O. M. Løvvik, S. M. Opalka, H. W. Brinks, and B. C. Hauback, *Phys. Rev. B* **69**, 134117 (2004).
- [5] B. C. Hauback, H. W. Brinks, C. M. Jensen, K. Murphy, and A. J. Maeland, *J. Alloys Compd.* **358**, 142 (2003).
- [6] B. C. Hauback, H. W. Brinks, R. H. Heyn, R. Blom, H. Fjellvåg, *J. Alloys Comp.* **394**, 35 (2005).
- [7] M. Fichtner, J. Engel, O. Fuhr, A. Gloss, O. Rubner, and R. Ahlrichs, *Inorg. Chem.* **42**, 7060 (2003).
- [8] O. M. Løvvik and P. N. Molin, *Phys. Rev. B* **72**, 073201 (2005).
- [9] M. Palumbo, F. J. Torres, J. R. Ares, C. Pisani, J. F. Fernandez and M. Baricco, *Calphad* **31** 457 (2007).
- [10] C. Wolverton and V. Ozolins, *Phys. Rev. B* **75**, 064101 (2007).
- [11] B. Bogdanovic, M. Schwickardi, *J. Alloys Compd.* **253**, 1 (1997).
- [12] A. Zaluska, L. Zaluski, J. O. Ström-Olsen, *J. Alloys Compd.* **298**, 125 (2000).
- [13] S. M. Opalka, D. L. Anton, *J. Alloys Compd.* **356-357**, 486 (2003).
- [14] H. Morioka, K. Kakizaki, S.-C. Chung and A. Yamada, *J. Alloys Comp.* **353**, 310 (2003).
- [15] P. Vajeeston, P. Ravindran, A. Kjekshus, H. Fjellvåg, *J. Alloys Comp.* **363**, L7 (2004).
- [16] A. Pommerin, A. Wosylus, M. Felderhoff, F. Schüth, and C. Weidenthaler, *Inorg. Chem.* **51**, 4143 (2012).
- [17] M. Amsler, J. A. Flores-Livas, T. D. Huan, S. Botti, M. A. L. Marques, and S. Goedecker, *Phys. Rev. Lett.* **108**, 205505 (2012).
- [18] J. K. Kang, J. Y. Lee, R. P. Muller, and W. A. Goddard, *J. Chem. Phys.* **121**, 10623 (2004).
- [19] T. N. Dymova, D. P. Aleksandrov, V. N. Konoplev, T. A. Siliana, and A. S. Sizareva, *Russ. J. Coord. Chem.* **20**, 263 (1994).
- [20] T. N. Dymova, D. P. Aleksandrov, V. N. Konoplev, T. A. Silina, and A. S. Sizareva, *Russ. J. Coord. Chem.* **20**, 279 (1994).
- [21] O. M. Løvvik and O. Swang, *J. Mater. Res.* **20**, 3199 (2005).
- [22] P. Vajeeston, P. Ravindran, A. Kjekshus, and H. Fjellvåg, *Phys. Rev. B* **69**, 020104 (2004).
- [23] E. Rönnebro, D. Noréus, K. Kadir, A. Reiser, B. Bogdanovic, *J. Alloys Comp.* **299**, 101 (2000).
- [24] M. Fichtner, C. Frommen, and O. Fuhr, *Inorg. Chem.* **44** 3479 (2005).
- [25] M. Mamatha, B. Bogdanovic, M. Felderhoff, A. Pommerin, W. Schmidt, F. Schüth, and C. Weidenthaler, *J. Alloys Compd.* **407**, 78 (2006).
- [26] T. N. Dymova, V. N. Konoplev, A. S. Sizareva, and D. P. Aleksandrov, *Russ. J. Coord. Chem.* **26**, 531 (2000).
- [27] A. Klaveness, P. Vajeeston, P. Ravindran, H. Fjellvåg, and A. Kjekshus, *J. Alloys Comp.* **433**, 225 (2007).
- [28] P. Hohenberg and W. Kohn, *Phys. Rev.* **136**, B864 (1964).
- [29] W. Kohn and L. Sham, *Phys. Rev.* **140**, A1133 (1965).
- [30] X. Gonze, B. Amadon, P.-M. Anglade, J.-M. Beuken, F. Bottin, P. Boulanger, F. Bruneval, D. Caliste, R. Caracas, M. Cote, T. Deutsch, L. Genovese, Ph. Ghosez, M. Giantomassi, S. Goedecker, D.R. Hamann, P. Hermet, F. Jollet, G. Jomard, S. Leroux, M. Mancini, S. Mazevet, M. J. T. Oliveira, G. Onida, Y. Pouillon, T. Rangel, G.-M. Rignanese, D. Sangalli, R. Shaltaf, M. Torrent, M. J. Verstraete, G. Zerah, and J. W. Zwanziger, *Computer Phys. Commun.* **180**, 2582 (2009).
- [31] X. Gonze, G.-M. Rignanese, M. Verstraete, J.-M. Beuken, Y. Pouillon, R. Caracas, F. Jollet, M. Torrent, G. Zerah, M. Mikami, Ph. Ghosez, M. Veithen, J.-Y. Raty, V. Olevano, F. Bruneval, L. Reining, R. Godby, G. Onida, D.R. Hamann, and D.C. Allan, *Zeit. Kristallogr.* **220**, 558 (2005).
- [32] X. Gonze and C. Lee, *Phys. Rev. B* **55**, 10355 (1997).
- [33] J. P. Perdew, K. Burke, and M. Ernzerhof, *Phys. Rev. Lett.* **77**, 3865 (1996).
- [34] C. Hartwigsen, S. Goedecker, and J. Hutter, *Phys. Rev. B* **58**, 3641 (1998).
- [35] H. J. Monkhorst and J. D. Pack, *Phys. Rev. B* **13**, 5188 (1976).
- [36] J. P. Perdew, A. Ruzsinszky, G. I. Csonka, O. A. Vydrov, G. E. Scuseria, L. A. Constantin, X. Zhou, and K. Burke, *Phys. Rev. Lett.* **100**, 136406 (2008).
- [37] S. Goedecker, *J. Chem. Phys.* **120**, 9911 (2004).
- [38] M. Amsler and S. Goedecker, *J. Chem. Phys.* **133**, 224104 (2010).
- [39] W. Hellmann, R. G. Hennig, S. Goedecker, C. J. Umrigar, B. Delley and T. Lenosky, *Phys. Rev. B* **75**, 085411 (2007).
- [40] S. Roy, S. Goedecker, M. J. Field and E. Penev, *J. Phys. Chem. B* **113**, 7315 (2009).
- [41] K. Bao, S. Goedecker, K. Koga, F. Lançon, and A. Neelov, *Phys. Rev. B* **79**, 041405 (2009).
- [42] A. Willand, M. Gramzow, S. Alireza Ghasemi, L. Genovese, T. Deutsch, K. Reuter, and S. Goedecker, *Phys. Rev. B* **81**, 201405 (2010).
- [43] S. De, A. Willand, M. Amsler, P. Pochet, L. Genovese, and S. Goedecker, *Phys. Rev. Lett.* **106**, 225502 (2011).
- [44] M. Amsler, J. A. Flores-Livas, L. Lehtovaara, F. Balima, S. A. Ghasemi, D. Machon, S. Pailhès, A. Willand, D. Caliste, S. Botti, A. San Miguel, S. Goedecker, M. A. L. Marques, *Phys. Rev. Lett.* **108**, 065501 (2012).
- [45] J. A. Flores-Livas, M. Amsler, T. J. Lenosky, L. Lehtovaara, S. Botti, M. A. L. Marques, and S. Goedecker, *Phys. Rev. Lett.* **108**, 117004 (2012).
- [46] See supplemental material for additional information reported in this work.
- [47] L. Hedin, *Phys. Rev.* **139**, A796 (1965).

Supplemental Material: Low-Energy Polymeric Phases of Alanates

Tran Doan Huan,¹ Maximilian Amsler,¹ Miguel A. L. Marques,²

Silvana Botti,² Alexander Willand,¹ and Stefan Goedecker¹

¹*Department of Physics, Universität Basel, Klingelbergstrasse 82, 4056 Basel, Switzerland*

²*Université de Lyon, F-69000 Lyon, France and LPMC, CNRS,*

UMR 5586, Université Lyon 1, F-69622 Villeurbanne, France

(Dated: November 6, 2012)

TABLE I: Crystallographic information of the polymeric phases of LiAlH_4 , NaAlH_4 , KAlH_4 , $\text{Mg}(\text{AlH}_4)_2$, $\text{Ca}(\text{AlH}_4)_2$, and $\text{Sr}(\text{AlH}_4)_2$ reported in Table 1 of the text. Three polymeric phases of LiAlH_4 were taken from Amsler *et. al*, Phys. Rev. Lett. **108**, 205505 (2012). The reference structure of $\text{Sr}(\text{AlH}_4)_2$, which is isolated, is also given. For each structure, cell parameters are given while for each atom, the Wyckoff site and the coordinates (x , y , and z) are given.

Lithium alanate LiAlH_4	
$P2_1/c$ (14)	$a = 5.16\text{\AA}$, $b = 4.27\text{\AA}$, $c = 5.09\text{\AA}$ $\alpha = 90^\circ$, $\beta = 66.84^\circ$, $\gamma = 90^\circ$
Li	(2b) (0.50000, 0.00000, 0.00000)
Al	(2c) (0.00000, 0.00000, 0.50000)
H	(4e) (0.13078, 0.27635, -0.31938)
H	(4e) (-0.31571, 0.17575, -0.37421)
$P2_1$ (4)	$a = 8.95\text{\AA}$, $b = 4.26\text{\AA}$, $c = 5.65\text{\AA}$ $\alpha = 90^\circ$, $\beta = 72.14^\circ$, $\gamma = 90^\circ$
Li	(2a) (0.37457, -0.28106, -0.06011)
Li	(2a) (-0.12448, -0.28716, 0.17209)
Al	(2a) (0.12440, 0.21972, 0.31117)
Al	(2a) (-0.37431, 0.21172, -0.44005)
H	(2a) (0.22067, 0.41391, 0.05002)
H	(2a) (-0.27624, 0.43397, -0.26465)
H	(2a) (-0.02773, -0.47771, -0.14545)
H	(2a) (-0.47225, -0.00521, 0.38450)
H	(2a) (-0.22202, -0.08255, -0.49578)
H	(2a) (-0.46952, 0.03961, -0.17022)
H	(2a) (0.27794, -0.11397, -0.29145)
H	(2a) (-0.02591, -0.48353, 0.40997)
$Pnc2$ (30)	$a = 4.75\text{\AA}$, $b = 4.22\text{\AA}$, $c = 5.10\text{\AA}$ $\alpha = \beta = \gamma = 90^\circ$
Li	(2b) (0.50000, 0.00000, 0.33423)
Al	(2a) (0.00000, 0.00000, -0.35590)
H	(4c) (0.14407, 0.25389, -0.11765)
H	(4c) (-0.30273, 0.20155, -0.38289)
Sodium alanate NaAlH_4	
$C2/m$ (12)	$a = 15.24\text{\AA}$, $b = 3.50\text{\AA}$, $c = 5.39\text{\AA}$ $\alpha = 90^\circ$, $\beta = 107.56^\circ$, $\gamma = 90^\circ$
Na	(4i) (-0.34347, 0.00000, -0.24813)
Al	(4i) (-0.08953, 0.00000, -0.16280)
H	(4i) (0.14076, 0.00000, 0.48462)
H	(4i) (-0.02391, 0.00000, 0.18320)
H	(4i) (-0.18490, 0.00000, -0.06296)
H	(4i) (0.41686, 0.00000, -0.14113)
$P1$ (2)	$a = 5.11\text{\AA}$, $b = 6.60\text{\AA}$, $c = 4.43\text{\AA}$ $\alpha = 88.82^\circ$, $\beta = 90.50^\circ$, $\gamma = 111.19^\circ$
Na	(2i) (0.38439, -0.29274, -0.15606)
Al	(2i) (-0.01100, -0.12960, 0.25799)
H	(2i) (0.19398, -0.03107, -0.07664)
H	(2i) (0.21437, -0.24151, 0.38794)
H	(2i) (-0.19577, -0.13495, -0.41092)
to be continued ..	

TABLE I – continued from previous page

H	(2i) (-0.24437, -0.34895, 0.09836)
$C2$ (5)	$a = 10.54\text{\AA}$, $b = 6.52\text{\AA}$, $c = 4.42\text{\AA}$ $\alpha = 90^\circ$, $\beta = 112.70^\circ$, $\gamma = 90^\circ$
Na	(4c) (0.20281, 0.30470, -0.39229)
Al	(2b) (0.00000, -0.16513, 0.50000)
Al	(2a) (0.00000, -0.42516, 0.00000)
H	(4c) (-0.40240, 0.11790, 0.42446)
H	(4c) (-0.38550, 0.49384, 0.45075)
H	(4c) (0.40619, 0.28509, 0.08137)
H	(4c) (0.11308, 0.40560, -0.03366)
Potassium alanate KAlH_4	
$P1$ (2)	$a = 6.70\text{\AA}$, $b = 4.45\text{\AA}$, $c = 6.06\text{\AA}$ $\alpha = 92.75^\circ$, $\beta = 68.97^\circ$, $\gamma = 72.32^\circ$
K	(2i) (-0.34460, -0.40015, -0.31700)
Al	(2i) (-0.12691, -0.18304, 0.10928)
H	(2i) (0.15276, -0.15067, 0.04133)
H	(2i) (-0.37153, -0.22773, 0.12201)
H	(2i) (0.02012, -0.44186, -0.18993)
H	(2i) (-0.23324, 0.03462, 0.38658)
$Ama2$ (40)	$a = 7.82\text{\AA}$, $b = 15.17\text{\AA}$, $c = 5.67\text{\AA}$ $\alpha = \beta = \gamma = 90.00^\circ$
K	(4b) (0.25000, 0.07042, -0.00532)
K	(4b) (0.25000, 0.27536, -0.49053)
Al	(8c) (0.41240, 0.39549, 0.02217)
H	(4b) (0.25000, 0.30881, -0.00499)
H	(8c) (0.47811, 0.13427, 0.28331)
H	(8c) (0.02473, -0.34359, 0.23133)
H	(4a) (0.00000, 0.00000, -0.42383)
H	(4b) (0.25000, 0.44890, -0.15423)
H	(4b) (0.25000, -0.07369, -0.25928)
$Cmcm$ (63)	$a = 3.67\text{\AA}$, $b = 11.86\text{\AA}$, $c = 7.19\text{\AA}$ $\alpha = \beta = \gamma = 90.00^\circ$
K	(4c) (0.00000, -0.30665, 0.25000)
Al	(4a) (0.00000, 0.00000, 0.00000)
H	(4b) (0.00000, 0.50000, 0.00000)
H	(8f) (0.00000, 0.14136, -0.00402)
H	(4c) (0.00000, 0.00829, 0.25000)
Magnesium alanate $\text{Mg}(\text{AlH}_4)_2$	
$P2_1$ (4)	$a = 4.51\text{\AA}$, $b = 4.55\text{\AA}$, $c = 9.98\text{\AA}$ $\alpha = 90.00^\circ$, $\beta = 101.96^\circ$, $\gamma = 90.00^\circ$
Mg	(2a) (0.29512, -0.02634, -0.40274)
Al	(2a) (0.24390, 0.22281, -0.00022)
Al	(2a) (-0.15399, 0.47331, -0.29219)
H	(2a) (0.38636, -0.31990, 0.29310)
H	(2a) (-0.42226, -0.36043, -0.42744)
H	(2a) (-0.05889, 0.39831, 0.03577)
H	(2a) (0.13407, 0.30705, -0.17280)
H	(2a) (-0.44962, 0.04055, -0.03447)
H	(2a) (0.33498, 0.13731, 0.17300)
H	(2a) (-0.08015, 0.26546, 0.29238)
to be continued ..	

TABLE I – continued from previous page

H	(2a) (0.01015, -0.19229, 0.42758)
<i>P2</i> (3)	$a = 4.48\text{\AA}$, $b = 5.31\text{\AA}$, $c = 4.41\text{\AA}$ $\alpha = 90.00^\circ$, $\beta = 92.67^\circ$, $\gamma = 90.00^\circ$
Mg	(1d) (0.50000, -0.33533, 0.50000)
Al	(1a) (0.00000, -0.09108, 0.00000)
Al	(1c) (0.50000, 0.21369, 0.00000)
H	(2e) (0.32816, -0.06011, -0.22224)
H	(2e) (0.33807, 0.41064, -0.24975)
H	(2e) (0.15455, -0.30170, 0.24011)
H	(2e) (0.18354, 0.15639, 0.19890)
<i>C2/m</i> (12)	$a = 8.89\text{\AA}$, $b = 10.86\text{\AA}$, $c = 4.42\text{\AA}$ $\alpha = 90.00^\circ$, $\beta = 92.03^\circ$, $\gamma = 90.00^\circ$
Mg	(4h) (0.00000, -0.35319, 0.50000)
Al	(4i) (0.26981, 0.00000, 0.00411)
Al	(4g) (0.00000, -0.13584, 0.00000)
H	(8j) (0.08219, 0.23232, 0.24755)
H	(8j) (0.16431, 0.38456, -0.22268)
H	(4i) (-0.08071, 0.00000, -0.21114)
H	(4i) (0.40761, 0.00000, -0.26730)
H	(8j) (-0.33887, 0.39048, -0.19922)
Calcium alanate $\text{Ca}(\text{AlH}_4)_2$	
<i>P2₁/c</i> (14)	$a = 4.16\text{\AA}$, $b = 4.16\text{\AA}$, $c = 11.95\text{\AA}$ $\alpha = 90.00^\circ$, $\beta = 108.40^\circ$, $\gamma = 90.00^\circ$
Ca	(2a) (0.00000, 0.00000, 0.00000)
Al	(4e) (-0.28230, 0.14675, -0.30741)
H	(4e) (-0.48587, 0.37669, -0.41016)
H	(4e) (-0.42854, 0.14663, 0.30279)
H	(4e) (0.02899, 0.04501, 0.19849)
H	(4e) (0.08832, 0.01889, 0.40979)
<i>C2</i> (5)	$a = 12.06\text{\AA}$, $b = 4.10\text{\AA}$, $c = 4.19\text{\AA}$ $\alpha = 90.00^\circ$, $\beta = 81.76^\circ$, $\gamma = 90.00^\circ$
Ca	(2a) (0.00000, 0.25891, 0.00000)
Al	(4c) (0.30667, 0.43109, -0.28675)
H	(4c) (-0.41202, 0.25256, 0.11586)
H	(4c) (-0.30321, 0.15498, -0.40771)
H	(4c) (-0.09489, 0.18145, -0.48305)
H	(4c) (-0.19922, 0.22039, 0.04385)
<i>Pm</i> (6)	$a = 6.56\text{\AA}$, $b = 7.64\text{\AA}$, $c = 4.24\text{\AA}$ $\alpha = 90.00^\circ$, $\beta = 108.40^\circ$, $\gamma = 90.00^\circ$
Ca	(1a) (-0.21687, 0.00000, 0.45419)
Ca	(1b) (0.49695, 0.50000, 0.30495)
Al	(2c) (0.31678, 0.17579, -0.41342)
Al	(2c) (-0.03929, 0.32428, -0.08756)
H	(2c) (-0.20211, -0.32774, -0.48443)
H	(2c) (0.11848, -0.16737, -0.21910)
H	(1a) (0.45169, 0.00000, -0.16278)
H	(2c) (0.44972, -0.34772, -0.19560)
H	(2c) (0.15901, 0.33247, 0.30057)
H	(2c) (-0.17261, 0.15243, -0.00059)
H	(2c) (0.48025, -0.17230, 0.34956)
H	(1a) (0.16273, 0.00000, 0.35438)
H	(1b) (-0.17406, 0.50000, 0.03291)

H (1b) (0.11440, 0.50000, -0.16883)

Strontium alanate $\text{Sr}(\text{AlH}_4)_2$

<i>Pm</i> (6)	$a = 6.72\text{\AA}$, $b = 7.81\text{\AA}$, $c = 4.37\text{\AA}$ $\alpha = 90.00^\circ$, $\beta = 72.05^\circ$, $\gamma = 90.00^\circ$
Sr	(1a) (0.21662, 0.00000, 0.34191)
Sr	(1b) (-0.49047, 0.50000, 0.17763)
Al	(2c) (-0.31192, 0.17411, -0.27840)
Al	(2c) (0.03366, 0.32565, 0.05810)
H	(2c) (0.18921, -0.32914, 0.29460)

to be continued ..

TABLE I – continued from previous page

H	(2c) (-0.12429, -0.17298, 0.34016)
H	(1a) (-0.44681, 0.00000, -0.39065)
H	(2c) (-0.44381, -0.34081, -0.36133)
H	(2c) (-0.15378, 0.32725, -0.14631)
H	(2c) (0.16481, 0.15860, -0.14952)
H	(2c) (-0.46680, -0.17064, 0.10502)
H	(1a) (-0.15983, 0.00000, -0.20754)
H	(1b) (0.16982, 0.50000, -0.17830)
H	(1b) (-0.11881, 0.50000, 0.27395)
<i>P2₁/c</i> (14)	$a = 10.74\text{\AA}$, $b = 4.52\text{\AA}$, $c = 12.07\text{\AA}$ $\alpha = 90.00^\circ$, $\beta = 23.64^\circ$, $\gamma = 90.00^\circ$
Sr	(2b) (0.50000, 0.00000, 0.00000)
Al	(4e) (0.24591, -0.41234, -0.00240)
H	(4e) (0.44015, 0.48321, -0.04678)
H	(4e) (0.48947, -0.40468, 0.30376)
H	(4e) (0.05630, -0.19912, -0.46170)
H	(4e) (-0.01740, 0.20644, -0.27913)
<i>P1</i> (2)	$a = 4.45\text{\AA}$, $b = 5.86\text{\AA}$, $c = 4.46\text{\AA}$ $\alpha = 82.96^\circ$, $\beta = 93.91^\circ$, $\gamma = 104.60^\circ$
Sr	(1h) (0.50000, 0.50000, 0.50000)
Al	(2i) (0.20564, -0.13595, 0.04876)
H	(2i) (-0.30539, 0.37303, 0.05150)
H	(2i) (-0.14144, -0.13990, -0.15458)
H	(2i) (0.42050, 0.05774, -0.24357)
H	(2i) (-0.05548, 0.28437, -0.37319)

Reference (isolated) structure for strontium alanate $\text{Sr}(\text{AlH}_4)_2$

<i>P1</i> (2)	$a = 7.34\text{\AA}$, $b = 6.61\text{\AA}$, $c = 6.44\text{\AA}$ $\alpha = 116.83^\circ$, $\beta = 77.81^\circ$, $\gamma = 82.93^\circ$
Sr	(2i) (-0.22657, -0.43364, 0.33412)
Al	(2i) (0.26651, 0.11974, -0.04604)
Al	(2i) (0.25319, -0.26007, 0.35768)
H	(2i) (0.07338, -0.34867, 0.47080)
H	(2i) (0.19747, 0.02204, -0.48404)
H	(2i) (-0.28208, 0.36532, -0.06979)
H	(2i) (-0.07343, -0.30874, 0.00379)
H	(2i) (0.22755, -0.13838, -0.16011)
H	(2i) (0.42972, 0.15590, -0.23470)
H	(2i) (0.31926, 0.19379, 0.20751)
H	(2i) (0.42586, -0.40056, 0.40593)

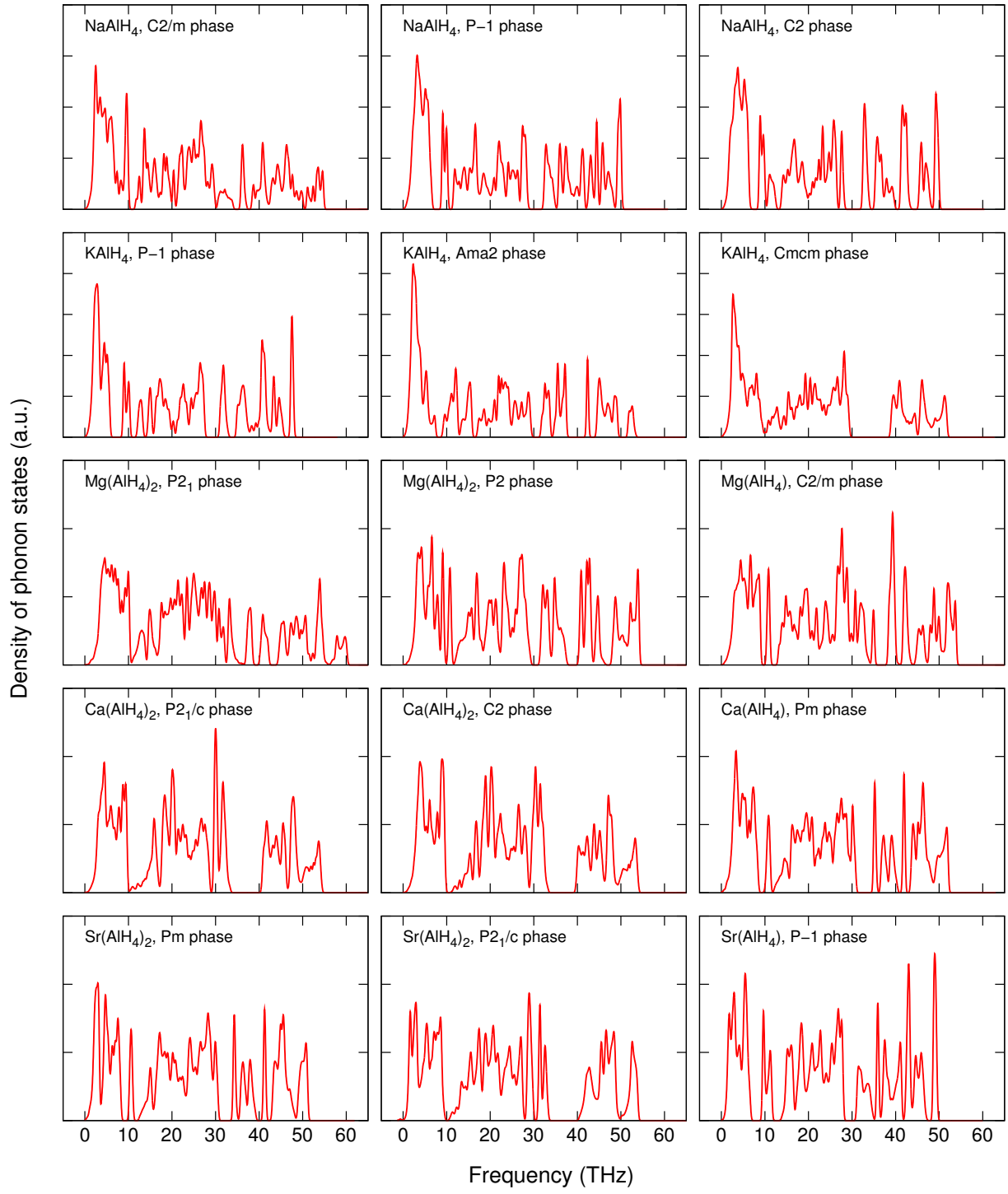


FIG. 1. (Color online) Densities of phonon states of three most stable polymeric phases of NaAlH₄, KAlH₄, Mg(AlH₄)₂, Ca(AlH₄)₂, and Sr(AlH₄)₂.

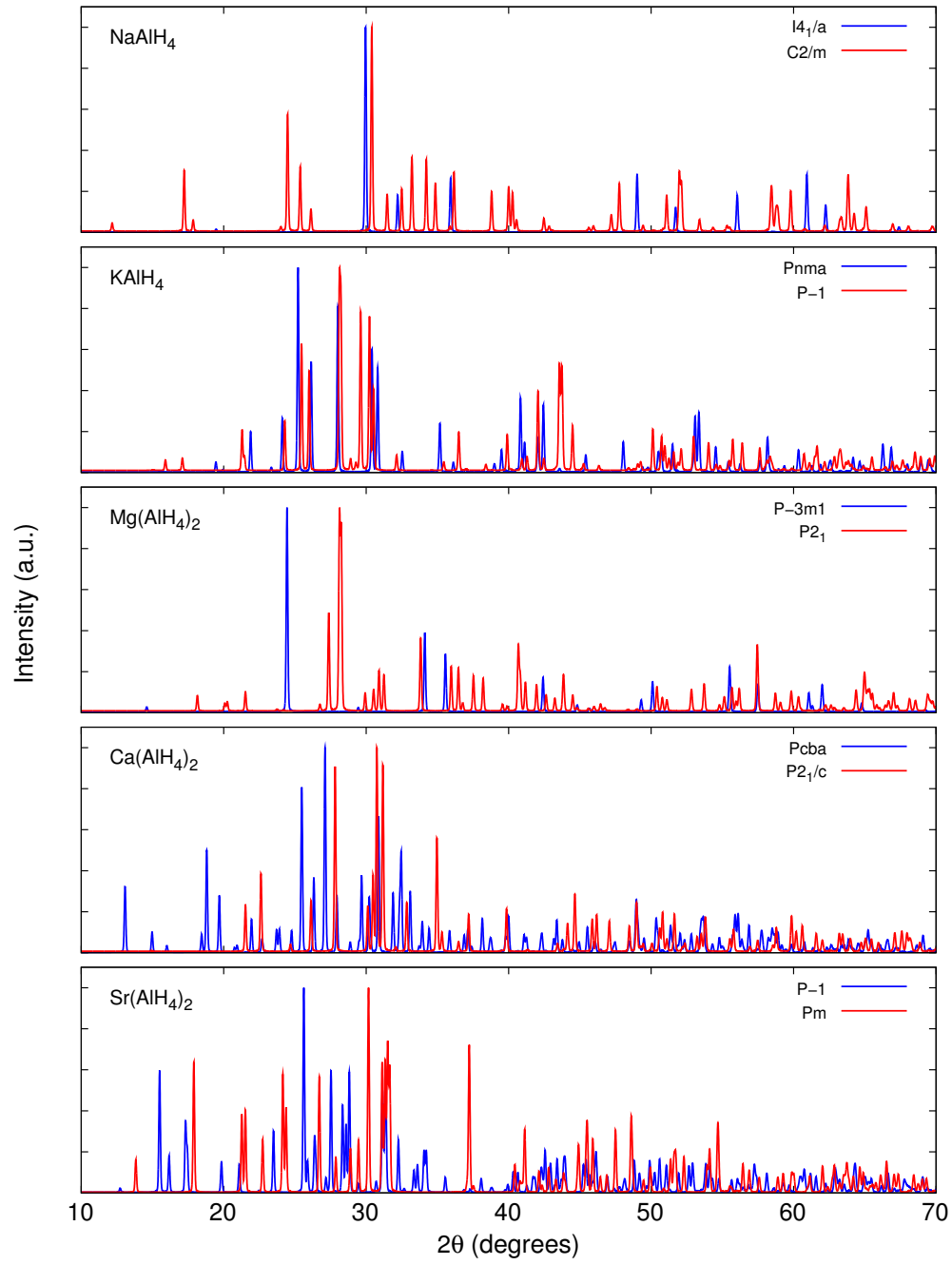


FIG. 2. (Color online) Simulated X-ray diffraction spectra of the most stable polymeric phases in a comparison with the corresponding reference isolated phases of NaAlH₄, KAlH₄, Mg(AlH₄)₂, Ca(AlH₄)₂, and Sr(AlH₄)₂.